View Article Online
View Journal

Environmental Science Nano

Accepted Manuscript

This article can be cited before page numbers have been issued, to do this please use: G. M. Newkirk, S. Jeon, H. Kim, S. Sivaraj, P. De Allende, C. Castillo, R. E. Jinkerson and J. P. Giraldo, *Environ. Sci.: Nano*, 2023, DOI: 10.1039/D3EN00268C.

ROYAL SOCIETY OF CHEMISTRY

rsc.li/es-nano

View Article Online
DOI: 10.1039/D3EN00268C

Environmental Significance Statement

Nanomaterial-mediated delivery of chemical and biomolecule cargoes into microbes can enable new methods and approaches for advancing biotechnology and synthetic biology. For example, transformation rates are a limiting factor for synthetic biology approaches in chloroplast biotechnology. New nanotechnology-based delivery approaches can positively impact renewable fuel production in algal biofuels, sustainable and biodegradable material production, and microbial fermenters and bioreactors. Orthogonally, nanomaterials such as single-walled carbon nanotubes are being released into the environment with unintended impacts. Runoff could affect photosynthetic microbial communities with a critical role in oxygen production for the atmosphere. Researching nanoparticle characteristics that impact uptake into photosynthetic microbes is crucial for developing more sustainable and renewable technologies.

View Article Online
DOI: 10.1039/D3EN00268C

DNA delivery by high aspect ratio nanomaterials to algal chloroplasts

Gregory M. Newkirk[1], Su-Ji Jeon[1], Hye-In Kim[1], Supreetha Sivaraj[1], Pedro De Allende[1], Christopher Castillo[1], Robert E. Jinkerson[2,3*], Juan Pablo Giraldo[1,2*]

[1]Department of Microbiology and Plant Pathology, University of California, Riverside, CA, USA

[2]Department of Botany and Plant Sciences, University of California, Riverside, CA, USA

[3]Department of Chemical and Environmental Engineering, University of California, Riverside, CA, USA

*** Correspondence:**

Corresponding Authors

juanpablo.giraldo@ucr.edu

robert.jinkerson@ucr.edu

Keywords: biotechnology, chloroplast, algae, carbon nanotubes, gene delivery.

Abstract

Chloroplast are sites of photosynthesis that have been bioengineered to produce food, biopharmaceuticals, and biomaterials. Current approaches for altering the chloroplast genome rely on inefficient DNA delivery methods, leading to low chloroplast transformation efficiency rates. For algal chloroplasts, there is no modifiable, customizable, and efficient *in situ* DNA delivery chassis. Herein, we investigated polyethylenimine-coated single-walled carbon nanotubes (PEI-SWCNT) as delivery vehicles for DNA to algal chloroplasts. We examined the impact of PEI-SWCNT charge and PEI polymer size (25k vs 10k) on the uptake into chloroplasts of wildtype and cell wall knockout mutant strains of the green algae *Chlamydomonas reinhardtii*. To assess the delivery of DNA bound

View Article Online
DOI: 10.1039/D3EN00268C

to PEI-SWCNT, we used confocal microscopy and colocalization analysis of chloroplast autofluorescence with fluorophore-labeled single-stranded GT_{15} DNA. We found that highly charged DNA-PEI25k-SWNCT have a statistically significant higher percentage of DNA colocalization events with algal chloroplasts (22.28% ± 6.42, 1 hr) over 1-3 hours than DNA-PEI10k-SWNCT (7.23% ± 0.68, 1 hr) ($P<0.01$). We determined the biocompatibility of DNA-PEI-SWCNT through assays for living algae cells, reactive oxygen species (ROS) generation, and *in vivo* chlorophyll assays. Through these assays, it was shown that algae exposed to DNA-PEI25k-SWCNT (30 fg/cell) and DNA-PEI10k-SWCNT (300 fg/cell) were viable over 4 days and had little impact on oxidative stress levels. DNA coated PEI-SWCNT transiently increased ROS levels within one hour of exposure to nanomaterials (30- 300 fg/cell) both in the wildtype strain and cell-wall knockout strain, followed by ROS decline to normal levels due to reaction with antioxidant glutathione and lipid membranes. PEI-SWCNT can act as biological carriers for delivering biomolecules such as DNA and have the potential to become novel tools for chloroplast biotechnology and synthetic biology.

1 Introduction

Algae biotechnology's applications range from the manufacturing of biodegradable bioplastics, renewable biofuels, and plant-based sustainable food sources.[1–3] Applied and basic research on algae biotechnology could be augmented by exploring emerging nanotechnology approaches. Potential applications of nanomaterials for algae biotechnology include gene delivery, biomolecule sensing, and enhancing photosynthetic efficiency[4–6] Single-walled carbon nanotubes (SWCNTs) have been shown to enter isolated chloroplasts,[7] plant protoplasts,[8] carry plasmid DNA *in planta* for the expression of green fluorescent proteins (GFP) in nuclei without genome integration[9] and enable chloroplast-specific expression in land plants.[10] SWCNTs are also capable of acting as near-infrared sensors for the detection of stress molecules, for example, by standoff monitoring of plant health though hydrogen peroxide sensing.[11] SWCNTs have also been shown to increase plant

View Article Online
DOI: 10.1039/D3EN00268C

photosynthetic efficiency by augmenting chloroplast light energy capture and conversion in plant leaves. [7]

Algae chloroplast biotechnology genetic advancements are currently being stymied by low chloroplast transformation rates due to non-specific and inefficient biomolecule delivery, limiting synthetic biology methods and applications.[12] In theory, each algal cell in a culture could be transformed, allowing for large phenotypic screening and directed evolution experiments using large mutant libraries. However, chloroplast transformation rates are a limiting step and major bottleneck for plastome bioengineering. For example, chloroplast transformation efficiency rates are so limiting for mutant library screening that directed evolution of Ribulose-1,5-bisphosphate carboxylase/oxygenase (RuBisCO) research is currently performed in bacteria.[13,14] The current standard protocol for the delivery of DNA for chloroplast transformation, particle bombardment, uses a microcarrier approach that, once tuned, is fairly universal across algae and plants. However, there are serious limitations with biomolecule delivery through particle bombardment: 1) the particles are unable to be targeted to specific parts of the cell, 2) cause cell and tissue damage, 3) a large amount of DNA is necessary, and 4) high cost of specialized equipment.[4,6] Therefore, there is justification for researching and applying new approaches for biomolecule delivery. Nanotechnology gene delivery approaches have been reported for land plants[9,10,15–17] but not for algae.

To date, the impact of high aspect ratio nanomaterials on algae, specifically of SWCNTs and multi-walled carbon nanotubes (MWCNTs), has been assessed through the guise of environmental toxicity. In photosynthetic green algae *Dunaliella tertiolecta, Pseudokirchneriella subcapitata,* and *Chlorella* exposure to MWCNTs or SWCNTs result in large aggregates of carbon nanotubes with consequent oxidative stress, low biocompatibility, and inhibition of growth.[18–22] The studies of nanomaterial applications to the algal model species *Chlamydomonas reinhardtii,* a staple of biology research for photosynthetic eukaryotic organisms, are limited to research focused on addressing

View Article Online
DOI: 10.1039/D3EN00268C

environmental toxicology questions. SWCNTs with no functionalization or coating were shown to have an inhibitory effect on growth, chlorophyll fluorescence, and quantum yield.[23] In contrast, salmon sperm DNA bound to sodium cholate-coated SWCNTs, at a 1:1 mass ratio, showed no inhibitory effect on *Chlamydomonas reinhardtii* growth or chlorophyll content at concentrations ranging from 0.1 to 100 μg/mL for an exposure duration of 10 days. [24] More recently, SWCNT have been reported to protect photosynthetic reactions in *Chlamydomonas* against photoinhibition.[25] Taken together, these results suggest that there is large potential in studying the nanotechnology applications for green algae and, specifically, the use of surface functionalized carbon nanotubes in *C. reinhardtii* for advancing biotechnology applications.

SWCNTs have been proposed to translocate across plant cell and chloroplast membranes by a lipid exchange envelope penetration (LEEP) mechanism.[26] The LEEP hypothesis posits that temporary pores are created in the chloroplast envelopes when the ionic cloud of highly charged nanomaterials disrupts the lipid membranes. The SWCNTs may become trapped within the outer and inner membranes of the chloroplast and become coated with membrane lipids.[7,26] Using fluorescence microscopy imaging of nanoparticles in extracted chloroplasts, the LEEP model was developed based on a nanoparticle's smallest size dimension and charge as the key factors influencing the translocation through plant lipid bilayers. Lew and colleagues expanded on the original LEEP hypothesis by looking at the uptake of nanoparticles into plant protoplasts via flow cytometry.[8] Specifically, the LEEP model hypothesizes that nanoparticles require +/- 20 mV to enter plant protoplasts and for entry into extracted chloroplasts ~+/-30 mV. It is hypothesized that a high concentration of carbon nanotubes could be lethal due to a higher frequency of contact between the nanoparticle and the lipid bilayer, causing an increase in membrane rupturing.[8,26] In algae, there are multiple obstacles that a nanoparticle must pass through before reaching the chloroplast membrane that were not considered by the LEEP model including the outer algae extracellular matrix and the

View Article Online
DOI: 10.1039/D3EN00268C

cell wall.[4] Semiconducting SWCNTs coated in ssDNA by pi-stacking interactions have been mapped inside plant and algae cells using Raman spectroscopy.[7,27] Due to highly stable and strong pi-stacking interactions, it is very unlikely that these DNA-SWCNT complexes are able to release DNA in organisms. In fact, this type of DNA-SWCNT has been shown to act as stable sensors for animal and plant biomolecules,[11,28,29] indicating the potential to act as tools to image and detect signaling molecules in algae. To date, no studies have investigated SWCNT mediated DNA delivery mechanisms into algae based on physical and chemical properties of nanomaterials. Our study elucidates DNA delivery mechanisms and biocompatibility in algae of oxidized SWCNTs coated by PEI through electrostatic interactions that have been shown to deliver and express transgene DNA in plants.[9,16]

This study focuses on understanding the impact of SWCNT charge and polyethylenimine (PEI) polymer size on the delivery of DNA to *Chlamydomonas* chloroplasts, measuring the effect of the algae cell wall barrier on SWCNT uptake, and SWCNT's influence on oxidative stress, chloroplast photosynthesis, and survivability **(Figure 1)**. We coated SWCNT with PEI varying in molecular weight (25k vs. 10k), a coating that has been previously shown to vary in charge and capable of delivering DNA biomolecules to land plants.[9,30] To determine if PEI-SWCNT coated with DNA (DNA-PEI-SWCNTs) entered into algae cells and chloroplasts, we used high spatial resolution confocal microscopy imaging for tracking a covalently bonded fluorophore to DNA cargo. To assess the impact of DNA-PEI-SWCNTs on *Chlamydomonas* oxidative stress, chloroplast photosynthesis and survivability, we measured the generation of reactive oxygen species (ROS), performed assays of glutathione antioxidant activity and lipid peroxidation, *in vivo* concentrations of chlorophyll and carotenoids, and live cell staining. This study advances our understanding of carbon nanotubes as a tool for nucleic acid delivery in microbial algae and the impact of high aspect ratio nanomaterials on algae function.

View Article Online
DOI: 10.1039/D3EN00268C

2 Results and discussion

2.1 Characterization of DNA-coated PEI-SWCNT

Carboxylated single-walled carbon nanotubes (COOH-SWCNTs, 5 nm d., Sigma-Aldrich, Cat# 652490-250MG) were dispersed into water, suspended in MES buffer (100 mM, pH 6), covered with a PEI coating of either of ~10,000 or ~25,000 molecular weight (PEI10k-SWCNT, PEI25k-SWCNT) through an EDC/NHS reaction, purified, and then finally bound to oligonucleotide DNA through a 30-minute binding reaction at room temperature. We analyzed the changes in height and length of COOH-SWCNTs after coating them with PEI and ssDNA via atomic force microscopy (AFM) (Figure 2a-d, S1). The AFM height for PEI25k-SWCNTs (7.60 ± 2.39 nm) was significantly larger (4.08 ± 1.83 nm, $p < 0.0001$) than that of COOH-SWCNTs but only slightly larger for PEI10k-SWCNTs (6.05 ± 1.83 nm, $p > 0.05$) (Figure 2c). AFM height for DNA-PEI10k-SWCNTs and DNA-PEI25k-SWCNTs increased to 13.13 ± 5.00 nm and 24.17 ± 9.13 nm ($p < 0.0001$), respectively (Figure 2c). In contrast, the average lengths of COOH-SWCNTs (0.87 ± 0.49 μm) decreased after being coated with PEI10k or PEI25k polymer to 0.67 ± 0.43 μm ($p < 0.05$) and 0.64 ± 0.26 μm ($p < 0.01$), respectively (Figure 2d). This can be attributed to a reduction in length during the tip sonication steps performed for suspending SWCNT coated in PEI. Coating PEI10k-/PEI25k -SWCNTs with DNA resulted in non-significant changes in length from 0.79 ± 0.24 μm to 0.82 ± 0.18 μm ($p > 0.05$) (Figure 2d). The AFM analysis showed that the thickness of PEI-SWCNT was increased by approximately 7 to 16 nm upon introduction of ssDNA, which is comparable with previous studies,[31] and suggested that the surface modification of SWCNTs with PEI 10k or PEI 20k polymer allowed DNA to bind to the surface.

We investigated the zeta potential and ssDNA binding of the nanomaterial complexes to optimize the ratio of DNA to PEI-SWCNTs. Both free DNA and COOH-SWCNT showed highly negative surface

View Article Online
DOI: 10.1039/D3EN00268C

charge of -42.6 ± 0.5 mV and -42.5 ± 0.7 mV respectively (**Figure 2e-f)**. Once coated with the positively charged PEI, it was observed that the surface charge of the SWCNTs changed to +14.5 ± 2.0 mV and +30.1 ± 2.0 mV for PEI10k-SWCNT and PEI-25k SWCNT, showing a narrow and single-peak shape, which indicated that the carbon nanotubes were successfully coated with these polymers (**Figure 2e-f, Table S1)**. Interestingly, the PEI-SWCNT zeta potential exhibited minimal change despite the progressive increase in DNA:PEI-SWCNT ratios from 0.01:1, 0.1:1 to 1:1 **(Table S1)**. These findings diverge from previously reported interactions involving PEI-SWCNT and dsDNA.[9,16] The observed disparity may be attributed to the distinctive structural properties of single-stranded DNA and plasmid DNA, and their arrangement on the PEI-SWCNT surface that influences the electric potential at the nanomaterial double layer. A DNA-loading assay was used to assess the amount of free GT_{15} oligonucleotide ssDNA that remained after a binding reaction of ssDNA with PEI10k-SWCNTs and PEI25k-SWCNTs at 0.01:1, 0.1:1, 1:1, and 10:1 DNA:PEI-SWCNT, respectively. This binding assay based on gel electrophoresis showed that 100% of DNA was loaded onto the PEI10k- and PEI25k-SWCNT through a 30-minute binding reaction (and further incubation of 1 hour) that mimics experimental conditions **(Figure S2)**. The narrow and single-peak shaped zeta potentials of DNA-PEI-SWCNT also indicated that all ssDNA had reacted with PEI-SWCNTs and there was no free ssDNA (**Figure 2e,f)**. Zeta potential measurements for DNA:PEI-SWCNT at 10:1 ratio could not be performed due to significant aggregation of the nanomaterial complexes. This ratio indicates the limits for loading of DNA on our PEI-SWCNT without leading to aggregation that could impair delivery of DNA and the nanomaterial complexes **(Figure S3)**. Together the zeta potential and ssDNA binding assays pointed out that the optimal reaction ratio was 1:1 DNA:PEI-SWCNT, where DNA adhered well without significant changes in the size of the complex. This 1:1 DNA:PEI-SWCNT ratio was subsequently used for the following experiments.

View Article Online
DOI: 10.1039/D3EN00268C

2.2 DNA delivery mediated by PEI-SWCNT in algae

We assessed the impact of the algal cell wall and differing PEI coatings of SWCNTs on Cy3-GT_{15} (Dye-DNA) delivery mediated by nanomaterials into chloroplasts. Wildtype algae (CC-124) and a cell wall knockout (CC-4533) were exposed to PEI10k-SWCNTs and PEI25k-SWCNTs (0.1 ng/uL), bound to Dye-DNA at a 1:1 mass ratio, and visualized by confocal microscopy **(Figure 3a,b)**; zoomed images for Dye-DNA delivered by PEI10k- and PEI25k-SWCNT to chloroplasts are also shown **(Figure S4-5)**. The highest rate of Dye-DNA uptake into the chloroplast was determined through colocalization analysis, upon 1 hour of exposure of both PEI10k and PEI25k-SWCNT (300 fg/cell, 1:1 Dye-DNA:SWCNT) with the wildtype and cell wall knockout strain **(Figure S6-8)**. The delivery of Dye-DNA by PEI25k-SWCNT significantly increased colocalization of Dye-DNA with chloroplasts compared to Dye-DNA-PEI10k-SWCNT in the cell wall knockout strain (****P<0.0001)**(Figure 3c)**. Orthogonal merged images indicate that after just 1 hour of incubation, Dye-DNA is being delivered and associated with the algae outer membrane and colocalizing with parts of the chloroplast with DNA-PEI10k-SWCNT and DNA-PEI2kk-SWCNT **(Figure 3a,b)**. Z-stacks were cell counted and analyzed for colocalization events and it was found that, with both the wildtype and cell knockout strain, DNA-PEI25k-SWCNT had a statistically significant increase in percentage of algae cells with Dye-DNA compared to DNA-PEI10k-SWCNT (****P<0.0001)**(Figure 3d)**. Both Dye-DNA-PEI10k-SWCNT and Dye-DNA-PEI25k-SWCNT (1-hour incubation) showed increased cell clumping, an indicator of algae experiencing stress or perhaps a result of electrostatic binding between Dye-DNA-PEI-SWCNT and algae cell walls **(Figure S7-8)**. A negative control of algae with Dye-DNA without PEI-SWCNTs was used for all confocal experiments to illustrate that the Dye-DNA does not associate with the algae unless the PEI-SWCNT is present **(Figure S9).** Overall, highly charged DNA-PEI25k-SWCNT (+30.6 ± 2.9 mV) are more effective than DNA-PEI10k-SWCNT (+17.0 ± 1.6 mV) at delivering DNA across algae biosurfaces

View Article Online
DOI: 10.1039/D3EN00268C

including the outer matrix, cell wall and lipid membranes into the chloroplasts as reported in land plant studies.[8,16,26]

Based on the LEEP model we expected the highly charged DNA-PEI25k-SWCNT (~30 mV) to deliver DNA into chloroplasts but not the lower charge (<20 mV) DNA-PEI10k-SWCNT. Both PEI25k and PEI10k SWCNTs are able to translocate and deliver DNA across multiple algae cell barriers including the extracellular matrix, cell wall, cell and organelle lipid membranes into chloroplasts. This indicates that the LEEP model has limitations for determining the delivery of DNA cargoes mediated by SWCNT into algae chloroplasts.[8,26] Nanomaterial translocation across algae extracellular matrix and cell wall was not tested by the LEEP model developed in plant protoplasts lacking cell walls.[8,26] Both the algae wildtype and the cell-wall knockout, CC-124 and CC-4533 with *cw15* phenotype, respectively, have a cell wall where the knockout has a highly reduced cell wall. CC-4533 is from a cross between 4A-, whose parental strain was CC-124, and D66+ which produces a *cw15* cell-wall knockout phenotype. [32,33] Chlamydomonas *cw15* phenotypes are produced from multiple genes and recent research has been unable to identify a genetic locus that produced that specific phenotype. [34] Entry of nanomaterials through these important algal biological surfaces and the biomolecule coronas that coat the particle thereafter have yet to be included in nanoparticle delivery models.[4] In addition, there is a significant drop in colocalization after 1 hour of incubation of the highly charged DNA-PEI25k-SWCNTs with the wildtype **(Figure S6)**. This is not expected from the LEEP hypothesis that proposes SWCNTs are kinetically trapped within cell lipid membranes after uptake. A possible explanation is that SWCNT is causing reduction in photosynthetic pigments and damage to organelles, as reported previously, [35,36] thus lowering colocalization rates with chloroplast pigments.

Future studies using plasmid DNA or DNA cassettes would allow assessing both delivery and expression of genes into algae chloroplasts mediated by PEI-SWCNTs. It remains to be determined if

View Article Online
DOI: 10.1039/D3EN00268C

this study using single-stranded DNA ($ssGT_{15}$) can be extrapolated to understand the delivery of plasmid DNA. A single fully intact molecule of dsDNA is capable of transforming the chloroplast genome, with plasmid DNA being the most compatible.[12] This study demonstrating the delivery of small DNA fragments (30 bp oligonucleotides, 300 fg/cell) across algae cell wall and membrane barriers highlights the potential of PEI-SWCNTs as carriers for plasmid DNA in microalgae. In comparison to our efficiencies for ssDNA delivery with PEI25k-SWCNT (35.22% ± 3.48 in the wildtype and 59.20% ± 2.17 in cell-wall knockout), particle bombardment, the current standard method for chloroplast transformation, has a 0.1-0.3% frequency of cells transiently expressing plasmid DNA after bombardment in cell culture suspensions. [37] Another future direction of this research could assist the delivery of RNA by PEI-SWCNTs in algae as it has been demonstrated using gold nanorods in plants.[38]

2.3 Effect of DNA-PEI-SWCNT on algae oxidative stress

Reactive oxygen species (ROS), shown previously to be a major contributor of nanomaterial toxicity to algae, were used as a metric to determine oxidative stress levels upon uptake of DNA-PEI-SWCNT. [35,39] The ROS levels were measured by interfacing algae with H_2DCF-DA (2′,7′-dichlorodihydrofluorescein-diacetate), a cell membrane permeable chemical that is cleaved by cellular esterases forming H_2DCF. The oxidation of H_2DCF by ROS in algae cells yields DCF (2′,7′-dichlorofluorescein). Wildtype algae experienced a significant increase in ROS levels within 2-hour exposure to 300 and 3000 fg/cell of DNA-PEI10k-SWCNTs ($P<0.005$, 2-way ANOVA). The ROS were maintained at similar levels to the control during the 3 hours exposure to the 30 fg/cell of DNA-PEI10k-SWCNTs treatment. In contrast, the 300 and 3000 fg/cell DNA-PEI10k-SWCNT treatment exhibited a significant increase in ROS levels that was followed by a steady decline over time ($P^{****}<0.0001$, 2-way ANOVA) **(Figure 4a)**. The DNA-PEI25k-SWCNTs showed a similar trend but with ROS levels increasing for the 30 fg/cell after 2 hr exposure and at a concentration of 3000

View Article Online
DOI: 10.1039/D3EN00268C

fg/cell after 1 hour, followed by a subsequent decline over time **(Figure 4b)**. The cell wall knockout strain had higher ROS generation levels than the wildtype and followed a similar trend of peaking ROS levels at 1 hour for both the PEI10k- and PEI25k-SWCNTs (300, and 3000 fg/cell), then declining ROS levels afterwards (P****<0.0001, 2-way ANOVA) **(Figure 4c,d)**. After 4 days, it was found that the cell wall knockout and wildtype strains had a statistically significant decrease in ROS with both the 300 fg/cell and 3000 fg/cell DNA-PEI10k-SWCNT and DNA-PEI25k-SWCNT (P***<0.001, P****<0.0001, respectively, 2-way ANOVA) **(Figure 4a,b)**. The larger increase in ROS levels in the cell wall knockout strain could be due to higher uptake of DNA-PEI-SWCNT compared to the wild type counterpart. Taken together, transient ROS levels increased after a 1 hour exposure of DNA-PEI-SWCNT but decreased over time, eventually leading to similar values as the negative controls.

The decline in ROS after exposure to DNA-PEI-SWCNT could be the result of ROS reaction with antioxidants or other biomolecules in algae cells upon increase in oxidative stress.[35] Glutathione is an antioxidant within algae cells that has been shown to be an important marker for toxicity screening and oxidative stress.[40–42] Intracellular reduced glutathione (GSH) is seen as a sensitive indicator of healthy cells and lower GSH can be interpreted as decreased cell health due to reaction with ROS. Monochlorobimane, mBCl, is a non-fluorescing cell permeable dye that reacts with intracellular GSH to become fluorescent bimane–glutathione.[41] After exposure to DNA-PEI10k-SWCNT and DNA-PEI25k-SWCNT, both wildtype and cell-wall knockout strains showed decreases in intracellular GSH **(Figure S10;** P<0.0001**),** an indicator that GSH was used to mitigate the impact of ROS in algae cells due to nanomaterial exposure.

To elucidate the effect of nanomaterial induced ROS generation on lipid membranes, a lipophilic fluorescent dye with a polyunsaturated butadienyl portion, BODIPY™ C11 undecanoic acid, was

View Article Online
DOI: 10.1039/D3EN00268C

exposed to the wildtype and cell-wall knockout strains as a lipid peroxidation assay.[43,44] Both PEI10k and PEI25k coatings (300 fg/cell and 1:1 DNA:PEI-SWCNT ratio by mass) produced statistically significant increases in lipid peroxidation in the wildtype and cell wall knockout strains in as little as one hour **(Figure S11)**. This lipid peroxidation assay indicates that ROS generated by the DNA-PEI-SWCNT damage lipid membranes compromising their integrity.

2.4 Effect of DNA-PEI-SWCNT on algae viability

For a population-based phenotypic assessment of the DNA-PEI-SWCNT impact on *Chlamydomonas reinhardtii* viability, we measured live cell viability staining, chlorophyll *a* and *b*, total carotenoids, and *in vivo* chlorophyll concentrations.[45–48] Fluorescein diacetate (FDA) was used as a fluorescence-based population-level viability indicator due to its wide use in *C. reinhardtii* research. [45] When exposed to the highest concentration of 3000 fg/cell DNA-PEI10k-SWCNTs or DNA-PEI25k-SWCNTs, the wildtype cell's viability dropped significantly over 2 and 3 hr (P****<0.0001, 2-way ANOVA) **(Figure 5a-b)**. The cell wall knockout showed a significant decrease in viability at lower concentrations of DNA-PEI SWCNT than the wildtype strain, after being exposed to 30 fg/cell DNA-PEI10k-SWCNTs over 1 and 2 hours (P****<0.0001, 2-way ANOVA) **(Figure 5c-d)**. Interestingly, wildtype strain exposure to both DNA-PEI10k-SWCNTs and DNA-PEI25k-SWCNTs resulted in a significant increase in FDA emission at 300 fg/cell starting at 1 hour (P**<0.001, P****<0.0001, respectively, 2-way ANOVA)**(Figure 5a-b).** Increasing concentrations of either DNA-PEI10k-SWCNTs or DNA-PEI25k-SWCNTs in the cell wall knockout also led to higher FDA emission levels than algae controls without nanomaterials. The DNA-PEI-SWCNTs may be facilitating the entry of other molecules besides the DNA cargoes into algae cells, causing higher FDA entry than algae-only samples. This may explain why there is higher FDA emissions from algae exposed to some concentrations of DNA-PEI10k-SWCNTs and DNA-PEI25k-SWCNTs. This

View Article Online
DOI: 10.1039/D3EN00268C

population-based FDA analysis also indicates a range of biocompatible concentrations (30-300 fg/cell) of highly charged PEI25k-SWCNT carrier for DNA delivery and the ability for the cell wall of algae to reduce the impact of DNA-PEI-SWCNT on algae viability.

Photosynthetic pigments of chlorophyll and carotenoids are parameters that assess changes in algal phenotype and photosynthesis. [49] The wildtype's chlorophyll *a* content dropped significantly with DNA-PEI10k-SWCNT at a concentration of 3000 fg/cell (P*<0.05, 2-way ANOVA) but the cell wall knockout was not affected **(Figure 6a)**. At 3000 fg/cell DNA-PEI25k-SWCNT, both the wildtype and cell wall knockout showed a significant decrease in the chlorophyll *a* compared to the algae-only control (P**<0.001, 2-way ANOVA)**(Figure 6b)**. The DNA-PEI10k-SWCNT caused no significant decreases in chlorophyll *b* levels for both the wildtype and cell wall knockout strain **(Figure 6c)**. However, both strains had no detectable chlorophyll *b* levels at 3000 fg/cell of DNA-PEI25k-SWCNT due to dead cells. A significant decrease between the 300 fg/cell of DNA-PEI25k-SWCNT and wildtype algae only controls was also observed (P***=0.0001, 2-way ANOVA)**(Figure 6d)**. No significant differences in total carotenoids of the algal cell were observed (P>0.9, 2-way ANOVA) in wildtype and cell wall knockout strains with DNA-PEI10k-SWCNT relative to controls without nanomaterials **(Figure 6e-f)**. However, wildtype and cell wall knockout algae exposed to DNA-PEI25k-SWCNTs at 3000 fg/cell showed significant differences in total carotenoids relative to algae-only controls (P*<0.003 for the cell wall knockout, P****<0.0001 for the wildtype, 2-way ANOVA). Overall, both DNA-PEI10k-SWCNTs and DNA-PEI25k-SWCNTs reduced chlorophyll pigments at 3000 fg/cell but DNA-PEI25k-SWCNTs had a larger impact on carotenoids than DNA-PEI10k-SWCNTs in a dose dependent manner. Based on both i*n vivo* chlorophyll and carotenoid content analysis over multiple days, 300 fg/cell of PEI10k-SWCNTs and 30 fg/cell of PEI25k-SWCNTs were deemed biocompatible with algal cultures. Previously, SWCNT directly coated with salmon testes genomic DNA by Π-stacking interactions at 1:1 mass ratio concentration were shown to be

View Article Online
DOI: 10.1039/D3EN00268C

biocompatible with *Chlamydomonas reinhardtii* wild-type strain (cc-1690) at concentrations from 0.1 to 100 μg/mL through growth curves and extracted chlorophyll *a* and *b*. [24] SWCNT have also been shown to protect against *Chlamydomonas reinhardtii* photosynthetic PSII inactivations and higher rates of photosynthetic electron transport. [25]

Overall, population-based assays of ROS for oxidative stress, FDA for living cells, and *in vivo* chlorophyll content all pointed to 300 fg/cell of DNA-PEI10k-SWCNT and 30 fg/cell of DNA-PEI25k-SWCNT being the concentrations that were deemed to be biocompatible with algal cultures. This study demonstrates that algae are able to survive upon exposure to nanomaterials (PEI-SWCNT) capable of delivering a biomolecule (DNA). The ROS, FDA and chlorophyll level analyses in combination with the glutathione and lipid peroxidation assays indicate that DNA-PEI-SWCNT mechanism of toxicity is increased oxidative stress and disruption of lipid membranes as they translocate into cell and chloroplast membranes.

3 Conclusions

This study demonstrates the application of engineered high aspect ratio nanomaterials for biomolecule delivery into algal chloroplasts. We showcased how the molecular weight of the PEI coating for SWCNTs impacts uptake into algae with and without a cell wall. In wild-type algae, the highly charged PEI25k-SWCNT showed higher potential for DNA delivery as evidenced by the higher colocalization rates of Dye-DNA with chloroplasts. We also identified biocompatible exposure conditions for delivery of DNA into *Chlamydomonas reinhardtii*. More than 300 fg/cell of the higher charged PEI25k-SWCNT showed higher lethality through the FDA cell viability assay, higher oxidative stress through the ROS assay, and no biocompatibility through the carotenoid assay. The biocompatibility assay for ROS showed lower generation for the wildtype algae with a cell wall, while the cell-wall knockout algae had higher oxidative stress levels for both PEI10k- and PEI25k-

View Article Online
DOI: 10.1039/D3EN00268C

SWCNTs. This highlights the role of the cell wall as a barrier for delivery of nanomaterials with biomolecule cargoes. The PEI-SWCNT mediated delivery of DNA into wildtype cells may lead to new opportunities for plasmid DNA delivery into chloroplasts.

This research into the intersection of nanotechnology and algae biotechnology opens new roads into biomolecule delivery and bioreactor productivity. Future research applications for PEI-coated SWCNTs could include coating with biorecognition peptide sequences for improved localization into chloroplasts. [17] Biomolecule delivery of genetic elements to algal chloroplasts can also enable the transient expression of genetic biosensors or synthetic riboswitches. [50] With one of the major bottlenecks of algae chloroplast transformation being DNA delivery efficiency and stable integration into chloroplasts, nanomaterial-mediated delivery could yield a higher number of genetic library mutants to be screened than current standard methods. [6] Taken together, these nanotechnology-based advancements in *Chlamydomonas* may also translate to other biofuel research-focused algae species. *Scenedesmus, Monoraphidium*, and *Pichoclorum* have been proposed as strong candidates for algae biofuel production. Nanotechnology approaches are providing tools for improving native photosynthetic performance, stress and health monitoring, and ROS as previously demonstrated in land plants.[5,7,11,51,52]

4 Materials and Methods

4.1 Algae Strain Culturing

Chlamydomonas reinhardtii wildtype strain, CC-124 and cell wall knockout strain, CC-4533 were ordered from the University of Minnesota Chlamy Center. All media contains Kropat's Trace Element mixture and TAP was used for liquid and solid culturing [53]. TAP plates supplemented with yeast extract at 4 g/L were used throughout to test for bacterial and yeast contamination. For strain maintenance, algae were grown with Bacto Agar (Cat#214010) at a 1.5% concentration under 50 μE

View Article Online
DOI: 10.1039/D3EN00268C

4K dimmable LED light conditions; a Walz ULM-500 was used to measure light intensity. For liquid culture, an orbital shaker (Cat#89032-100) at room temperature, with 150 rpm under a 100 PAR light with 24-hour photoperiod and Flytianmy drawer dividers were used to organize the shake flasks. All flasks were 50 mL Erlenmeyer flasks with Chemglass silicone sponge closure. Flasks and sponge closures were sterilized by autoclaving before the addition of TAP liquid media, and a second sterilization step of 121^{0}C for 20 minutes was performed to sterilize the TAP media.

4.2 Preparation of SWCNT with PEI and DNA Coating

All SWCNT preparation and PEI reaction steps are followed by previous studies unless otherwise noted [9,54]. An in-depth protocol reference is available with applicable troubleshooting steps [54]. A solution of COOH-SWCNT is made with 30 mg of dry COOH-SWCNT (Cat# 652490-250MG) and 30 mL molecular quality water (VWR, Cat# VWRL0201-0500), followed by 10-minute bath sonication. Once finished, samples were tip sonicated at 90% amplitude with the ThermoFisher (Model# FB120) and 6-mm probe tip (Model# CL-18) at ~30 W for 30-minutes in an ice bath. Mixtures were cooled for 10 minutes before ultracentrifugation (Beckman L8-60M) at 18,000 g for 1 hour at 20˚C. A pipette was used to remove the supernatant, carefully not disturbing the pellet, and leaving liquid at the bottom so as to not bring any clumped nanotubes into the next reaction. Using Beer-Lambert's Law (A = C * E * L) and a 1:10 dilution in water, the concentration of COOH-SWCNT was calculated using the absorbance value at 632 nm where E = 0.036 L/cm*mg and L = 1 cm. Typical concentration ranges are around 175 ± 25 mg/L. This solution can be stored for a month at room temperature.

AMES buffer solution was first prepared prior to reaction (500 mM, pH 4.5-5) . Next, a COOH-SWCNT solution was diluted to 100 mg/L. Then, 20 mL of the 100 mg/L COOH-SWCNT solution to a 50 mL conical tube for a final amount of 2 mg and 5 mL of the MES buffer was added to yield a

View Article Online
DOI: 10.1039/D3EN00268C

100 mM final concentration. Solution pH was then adjusted to be between 4.5 to 6 using HCl or NaOH as necessary. In a separate tube, 10 mg EDC and 10 mg NHS were added to 500 uL of 500 mM and 2 mL of molecular quality water and dissolved completely. EDC-NHS solutions were added dropwise to the COOH-SWCNT suspension while stirring, then bath sonicated for 15 minutes and placed on a 150 rpm orbital shaker for 45 minutes. Two 50 mL centrifugal 100,000-MWCO filters (Cat# UFC910024) were pre-washed with 15 mL of 0.1x PBS at 4,000g for 1 minute at room temperature.The COOH-SWCNT solution was then split between the two 50 mL centrifuge tubes and centrifuged at 300g for 8 min at 21˚C. Flow-through was discarded and volume was raised back up to the 50 mL line with 0.1x PBS. Solutions were briefly vortexed, and centrifuged again. This wash step was repeated two additional times to remove excess EDC and NHS. Both filtered solutions were then added to the same tube and filled to 20 mL before MES addition. This solution was bath sonicated for 15 minutes. In a new tube, 40 mg of PEI (PEI10k, Alfa Aesar Cat# 40331; PEI25k Sigma-Aldrich Cat# 408727-100ML) was added to a 15 mL conical tube and fully dissolved with 5 mL of 0.1x PBS. Solution's pH was then adjusted between 7.4 to 7.6. Lastly, activated COOH-SWCNT was added to the PEI solution in a dropwise manner while stirring. Reaction solution pH was then adjusted to between 7 and 8. The reaction solution was then placed on an orbital shaker at 150 rpm for 16 hours.

Two 100,000-MWCO 50 mL centrifugal filter tubes were washed with 15 mL nuclease-free water at maximum speed for 2 minutes. The PEI-SWCNT reaction mixture was split into both tubes, and centrifuged at 1,000g for 15 min at 21˚C. The flow-through was discarded, and the liquid level was brought back up to 15 mL with water, briefly vortexed, and centrifuged again. This wash was repeated 5 additional times. The liquid level was brought up to the previous level (20 mL as previously described). The solution was bath sonicated for 15-minutes, then tip sonicated for 15-minutes with a 6-mm tip in an ice bath at ~30% W, or 90% amplitude for 15 minutes; ice was

View Article Online
DOI: 10.1039/D3EN00268C

replaced halfway through this tip sonication. The solution was centrifuged at 18,000 rpm in an ultracentrifuge for 1-hour at room temperature, and pipetted off to not disturb the pellet. The solution was centrifuged with the same parameters two additional times to remove large PEI-SWCNT bundles. Beer-Lambert's Law was then used to calculate the concentration and continue to characterize this PEI-SWCNT solution. The solution can be kept at 4˚C for 1 month.

Coating GT_{15} and Cy3-GT_{15} onto the PEI-SWCNT was done by adding the corresponding concentration of DNA to the microcentrifuge tube first, adding the PEI-SWCNT dropwise, and finally pipetting up and down ten times. The binding reaction was allowed to go on at room temperature for 30 minutes before proceeding and being used.

4.3 Characterization of PEI-SWCNT and DNA-PEI-SWCNT

Characterization of the nanomaterials was done immediately after preparation. The nanomaterials can be used experimentally within 30 days if kept at 4 ℃. All PEI10k- and PEI25k- were diluted to 30 ng/uL and buffered with 10 mM TE final concentration for zeta potential, gel electrophoresis, and AFM measurements.

Beer-Lambert's Law was used to determine the concentration of SWCNT solution, using a spectrophotometer at 632 nm with a 1:10 dilution, where E = 0.036 L/cm*mg and L = 1 cm. A Malvern Nano-S was used for the zeta potential measurements with a specialized folded capillary cell (Model# DTS1070). All measurements were taken with a final concentration of 100 mM Tris-EDTA buffer. Twelve technical replicates were performed for each sample and the Henry model was used to measure zeta potential and pH measured between 7.4 to 7.5.

Standard gel electrophoresis was performed with 1% TBE gel, SYBR Safe (Cat# S33102), and Invitrogen 1 kb Plus DNA Ladder (Cat#10787018) for Dye-DNA binding assays to PEI-SWCNT. A

View Article Online
DOI: 10.1039/D3EN00268C

60 minute room temperature binding reaction was performed before adding DNA Gel Loading Dye (Cat#R0611) and running of the gel electrophoresis. Analysis of the bands for DNA binding efficiency was performed by GelAnalyzer 19.1.

AFM images of COOH-SWCNTs, and PEI-coated SWCNTs with and without DNA were collected by using a tapping mode with NanoScope 5000C-1 and analyzed with Gwyddion software. A total of 50 individual particles were measured for each sample type. DNA:PEI-SWCNT was bound at a mass ratio of 1:1, pipetted up and down ten times, and then incubated at room temperature for 30 minutes. The 15 uL mixture was then pipetted onto a silica wafer and let to dry at room temperature. The silica wafer was rinsed with distilled water three times, and dried at room temperature for 30 min before AFM measurements.

4.4 Dye-DNA-PEI-SWCNT Confocal Microscopy

The PEI-SWCNT solution was first bath sonicated in an Elmasonic P at 37 Hz for 30 minutes to disperse any bundles. Cy3-GT_{15} (Dye-DNA) was ordered and synthesized by IDT and then bound to PEI-SWCNTs at the appropriate mass ratio by adding the PEI-SWCNTs to the Dye-DNA dropwise, to reduce aggregation, and then pipetted up and down 10 times; this was performed at room temperature for 30 min. A liquid algae culture midway through exponential growth was then measured using OD_{550}. All experiments are done at an OD_{550} of 0.5. After the Dye-DNA has been bound to the PEI-SWCNT, algae are then added to the Dye-DNA-PEI-SWCNT solution dropwise in 1.7 mL tubes, and then pipetted up and down ten times. Wrap the tubes in foil to prevent any bleaching and put on an orbital shaker set to 150 rpm for the appropriate exposure time to be tested. Algae was then pelleted at 4000 g for 10 minutes and the supernatant was pipetted off, leaving around 10 µl. Pellet was then resuspended by gently pipetting up and down.

Algae samples were fixed on glass slides for confocal analysis using agarose pads (1%). In brief, 10

View Article Online
DOI: 10.1039/D3EN00268C

µl of room temperature chilled 1% agarose solution was mixed with 10 µl of algae pellet and was mixed by pipetting up and down. Mixture was then dispensed on a microscopy slide and covered using a cover slip. To fix the slide for long-term exposure experiments, nail polish was applied via pipette at the end to seal the sides and prevent evaporation.

On an inverted Zeiss 880 confocal microscope, 2 µm slices and 199 µm pinhole were used with a Cy3-DNA channel exciting with 2% of 514 nm laser and catching the emission from 538-589 nm. Additionally, a chloroplast autofluorescence channel exciting with 2% of 594 nm laser and emission range from 599-690 nm was simultaneously used. 200x was used to capture population-based images, captured in five random places on the slide for statistical significance. 1000x magnification was used to capture the z-stack analyses for confirmation at the organelle-level.

To calculate the thresholded Mander's coefficients for Dye-DNA delivered within chloroplasts in algae, we analyzed the overlap between chloroplast and Dye-DNA pixels using Fiji-ImageJ software. This coefficient was derived from the ratio of chloroplast pixels that colocalized with Dye-DNA to the total number of chloroplast pixels The signal threshold for Dye-DNA (15 for wildtype and 7 for cell-wall knockout strain) and chloroplast (27 for wildtype and 34 for cell-wall knockout strain) were set based on pixel values from algae samples without Dye-DNA within a pixel value range of 0-255. This method provided us with a more precise quantification of the Dye-DNA's location both within the chloroplast and throughout the algae.

4.5 Algal PEI-SWCNT *In Vivo* Biocompatibility Assays

A standard mass of DNA-PEI-SWCNT per algae cell (30 to 3000 fg/cell) was used with a concentration of DNA (1:1 ratio, ng/µL), PEI-SWCNT (5 ng/µL), and concentration of algae (OD_{550} = 0.100 = 1.49 x10^6 cells/mL) across assays. [45] The algae culture within a 96-well plate completes their growth curve at 4 days and enters into the death phase of the culture thereafter. Therefore,

View Article Online
DOI: 10.1039/D3EN00268C

biocompatibility assays were performed for up to 4 days of algae culture growth.

Population-based biocompatibility analysis for *Chlamydomonas* and DNA-PEI-SWCNT was performed with black opaque 96-well plates using fluorescein diacetate (FDA, Cat# F1303; ex: 493 nm, em: 523 nm) final concentration 2.4 μM (1μg/mL). After the 48-hour culture, samples were incubated in the dark for 30 minutes before sampling. Negative controls for cell viability were made by heating samples in a PCR machine for 45 minutes at 90˚C. Percent viability was calculated and OD_{550} was taken for cells/mL. In addition, 2′,7′-dichlorodihydrofluorescein diacetate (H_2DCFDA, Cat# D399; ex: 493 nm, em: 523 nm) at a final concentration of 100 μM (48.73 μg/mL) was used to measure the presence of ROS produced from the exposure to DNA-PEI-SWCNTs.

FDA diffuses across the cell membrane of the algae, and if the cell is alive, cytoplasmic esterases cleave FDA to produce anionic fluorescein, becoming excitable and capturable by a plate reader at a specific emission wavelength (λ_{ex} = 475 nm, λ_{em} = 535 nm). PEI-SWCNT was bound to GT_{15} DNA oligonucleotides without a fluorophore for these measurements, with the same room temperature binding reaction. The following plate reader-based culturing and *in vivo* phenotypic screens were adapted from Haire and colleagues [45]. Using the cells/mL polynomial, cells/ml polynomial =(216944)+(8483581*(OD550))+(46233132*(OD550^2))+(-36516574*(OD550^3)), cells were diluted to OD550 = 0.01 (~3x10^5 cells/mL). These cultures were then grown with 96-well plates at 200 μL for 48 hours under 50 PAR of continuous light on an orbital shaker at 150 rpm. All readings were taken on a Tecan Infinite M Plex with the following settings: 25 flashes, 16 square readings per plate, and 30 seconds of orbital shaking between rounds of readings with a 2 μm radius.

Using clear plates and the above culturing methods, photosynthetic photopigment analysis was performed to assess the impact of DNA-PEI-SWCNTs. After the 48-hour period, *in vivo* carotenoid concentrations were measured spectrophotometrically at 470, 550, 650, 680, and 750 nm (for

View Article Online
DOI: 10.1039/D3EN00268C

cells/mL). The acetone-based chlorophyll extraction was used by Lichtenthaler and colleagues. [45,55] The formula for Chlorophyll *a* was used: ChlA (µg/ml) = 12.25(A663)–2.79(A647); Chlorophyll *b*: ChlB (µg/ml) = 21.5(A647)–5.1(A663); and finally total carotenoid = [1000(A470)–1.82(ChlA)–85.02(ChlB)]/198.

Monochlorobimane (mBCl; Cat#: M1381MP; stock 50 mM in DMSO) was used to detect changes in intracellular reduced GSH levels and was added at a final concentration of 50 µM to both strains after 1 hour exposure to 300 fg/cell DNA-PEI-SWCNT in TAP buffer - in a 1:1 DNA:PEI-SWCNT mass ratio - then left to incubate in the dark while shaking for 1.5 hours. A black 96-well plate was used to record fluorescent bimane–glutathione (λ_{ex}: 405 nm, λ_{em}: 486 nm) on a plate reader (Tecan Infinite M Plex).

BODIPY™ 581/591 C11 undecanoic acid, 4,4-difluoro-5-(4-phenyl-1,3-butadienyl)-4-bora-3a,4a-diaza-s-indacene-3-undecanoic acid (Cat# D3861; λ_{ex}: 488 nm, λ_{em}: 510 nm; 50 mM stock solution diluted in DMSO), was used at a final concentration of 2 µg mL−1 to evaluate lipid peroxidation due to being oxidized by peroxyl radicals, which can be detected after excitation at 488 nm and an emission peak shift from 590 to 510 nm. PEI10k- and PEI25k-SWCNT was bound to DNA in a 1:1 ratio by mass, exposed to both strains at 300 fg/cell in TAP buffer, and measured in a plate reader with a black 96-well plate (Tecan Infinite M Plex).

5 Conflict of Interest

The authors declare that the research was conducted in the absence of any commercial or financial relationships that could be construed as a potential conflict of interest.

6 Author Contributions

View Article Online
DOI: 10.1039/D3EN00268C

G.M.N, J.P.G and R.E.J. conceived the idea and designed the experiments. G.M.N. performed most experiments including synthesis of nanomaterials, DNA delivery, ROS, FDA, and chloroplast pigment analysis. H.K. S.J. and C.C. performed nanoparticle characterizations and colocalization analysis. S.S. assisted biocompatibility assays and P.D.A. with confocal microscopy measurements. All authors contributed to writing the manuscript.

7 Funding

This work was supported by the National Science Foundation under the Center for Sustainable Nanotechnology, CHE-2001611. The CSN is part of the Centers for Chemical Innovation Program. G.M.N. was supported by a fellowship by the Department of Defense National Science and Engineering Graduate Fellowship Program. The authors are also grateful for funding from Frank G. and Janice B. Delfino Agricultural Technology Research Initiative.

8 Acknowledgments

All figures are made on Biorender.com.

9 References

1 P. Maliga and R. Bock, *Plant Physiol.*, 2011, **155**, 1501–1510.
2 S. Mayfield and S. S. Golden, *Photosynth. Res.*, 2015, **123**, 225–226.
3 C. Mathiot, P. Ponge, B. Gallard, J.-F. Sassi, F. Delrue and N. Le Moigne, *Carbohydr. Polym.*, 2019, **208**, 142–151.
4 G. M. Newkirk, P. de Allende, R. E. Jinkerson and J. P. Giraldo, *Front. Plant Sci.*, 2021, **12**, 1496.
5 J. P. Giraldo, H. Wu, G. M. Newkirk and S. Kruss, *Nat. Nanotechnol.*, 2019, **14**, 541–553.
6 J. W. Wang, E. G. Grandio, G. M. Newkirk, G. S. Demirer, S. Butrus, J. P. Giraldo and M. P. Landry, *Mol. Plant*, 2019.
7 J. P. Giraldo, M. P. Landry, S. M. Faltermeier, T. P. McNicholas, N. M. Iverson, A. A. Boghossian, N. F. Reuel, A. J. Hilmer, F. Sen, J. A. Brew and M. S. Strano, *Nat. Mater.*, 2014, **13**, 400–408.
8 T. T. S. Lew, M. H. Wong, S.-Y. Kwak, R. Sinclair, V. B. Koman and M. S. Strano, *Small*, 2018, e1802086.
9 G. S. Demirer, H. Zhang, J. L. Matos, N. S. Goh, F. J. Cunningham, Y. Sung, R. Chang, A. J. Aditham, L. Chio, M.-J. Cho, B. Staskawicz and M. P. Landry, *Nat. Nanotechnol.*, , DOI:10.1038/s41565-019-0382-5.
10 S.-Y. Kwak, T. T. S. Lew, C. J. Sweeney, V. B. Koman, M. H. Wong, K. Bohmert-Tatarev, K. D. Snell, J. S. Seo, N.-H. Chua and M. S. Strano, *Nat. Nanotechnol.*, , DOI:10.1038/s41565-019-0375-4.

View Article Online
DOI: 10.1039/D3EN00268C

11 H. Wu, R. Nißler, V. Morris, N. Herrmann, P. Hu, S.-J. Jeon, S. Kruss and J. P. Giraldo, *Nano Lett.*, 2020, **20**, 2432–2442.
12 R. Bock, *Annu. Rev. Plant Biol.*, 2015, **66**, 211–241.
13 R. H. Wilson, E. Martin-Avila, C. Conlan and S. M. Whitney, *J. Biol. Chem.*, 2018, **293**, 18–27.
14 G. Zhu, I. Kurek and L. Liu, in *The Chloroplast: Basics and Applications*, eds. C. A. Rebeiz, C. Benning, H. J. Bohnert, H. Daniell, J. K. Hoober, H. K. Lichtenthaler, A. R. Portis and B. C. Tripathy, Springer Netherlands, Dordrecht, 2010, pp. 307–322.
15 H. Zhang, G. S. Demirer, H. Zhang, T. Ye, N. S. Goh, A. J. Aditham, F. J. Cunningham, C. Fan and M. P. Landry, *Proc. Natl. Acad. Sci. U. S. A.*, 2019, **116**, 7543–7548.
16 I. Santana, S.-J. Jeon, H.-I. Kim, M. R. Islam, C. Castillo, G. F. H. Garcia, G. M. Newkirk and J. P. Giraldo, *ACS Nano*, , DOI:10.1021/acsnano.2c02714.
17 I. Santana, H. Wu, P. Hu and J. P. Giraldo, *Nat. Commun.*, 2020, **11**, 2045.
18 L. Wei, M. Thakkar, Y. Chen, S. A. Ntim, S. Mitra and X. Zhang, *Aquat. Toxicol.*, 2010, **100**, 194–201.
19 S. Youn, R. Wang, J. Gao, A. Hovespyan, K. J. Ziegler, J.-C. J. Bonzongo and G. Bitton, *Nanotoxicology*, 2012, **6**, 161–172.
20 Z. Long, J. Ji, K. Yang, D. Lin and F. Wu, *Environ. Sci. Technol.*, 2012, **46**, 8458–8466.
21 M. Thakkar, S. Mitra and L. Wei, *J. Nanomater.*, , DOI:10.1155/2016/8380491.
22 F. Schwab, T. D. Bucheli, L. P. Lukhele, A. Magrez, B. Nowack, L. Sigg and K. Knauer, *Environ. Sci. Technol.*, 2011, **45**, 6136–6144.
23 D. N. Matorin, A. V. Karateyeva, V. A. Osipov, E. P. Lukashev, N. K. Seifullina and A. B. Rubin, *Nanotechnol. Russ.*, 2010, **5**, 320–327.
24 R. M. Williams, H. K. Taylor, J. Thomas, Z. Cox, B. D. Dolash and L. J. Sooter, *J. Nanosci. Nanotechnol.*, , DOI:10.1155/2014/419382.
25 T. K. Antal, A. A. Volgusheva, G. P. Kukarskikh, E. P. Lukashev, A. A. Bulychev, A. Margonelli, S. Orlanducci, G. Leo, L. Cerri, E. Tyystjärvi and M. D. Lambreva, *Plant Physiol. Biochem.*, 2022, **192**, 298–307.
26 M. H. Wong, R. P. Misra, J. P. Giraldo, S.-Y. Kwak, Y. Son, M. P. Landry, J. W. Swan, D. Blankschtein and M. S. Strano, *Nano Lett.*, 2016, **16**, 1161–1172.
27 S. Orlanducci, G. Fulgenzi, A. Margonelli, G. Rea, T. K. Antal and M. D. Lambreva, *Materials* , , DOI:10.3390/ma13225121.
28 J. P. Giraldo, M. P. Landry, S.-Y. Kwak, R. M. Jain, M. H. Wong, N. M. Iverson, M. Ben-Naim and M. S. Strano, *Small*, 2015, **11**, 3973–3984.
29 N. M. Iverson, P. W. Barone, M. Shandell, L. J. Trudel, S. Sen, F. Sen, V. Ivanov, E. Atolia, E. Farias, T. P. McNicholas, N. Reuel, N. M. a. Parry, G. N. Wogan and M. S. Strano, *Nat. Nanotechnol.*, 2013, **8**, 873–880.
30 E. Martin-Avila, Y.-L. Lim, R. Birch, L. M. A. Dirk, S. Buck, T. Rhodes, R. E. Sharwood, M. V. Kapralov and S. M. Whitney, *Plant Cell*, 2020, **32**, 2898–2916.
31 Z. Ali, M. F. Serag, G. S. Demirer, B. Torre, E. di Fabrizio, M. P. Landry, S. Habuchi and M. Mahfouz, *ACS Appl. Nano Mater.*, 2022, **5**, 4663–4676.
32 R. M. Dent, C. M. Haglund, B. L. Chin, M. C. Kobayashi and K. K. Niyogi, *Plant Physiol.*, 2005, **137**, 545–556.
33 R. A. Schnell and P. A. Lefebvre, *Genetics*, 1993, **134**, 737–747.
34 S. D. Gallaher, S. T. Fitz-Gibbon, A. G. Glaesener, M. Pellegrini and S. S. Merchant, *Plant Cell*, 2015, **27**, 2335–2352.
35 F. Chen, Z. Xiao, L. Yue, J. Wang, Y. Feng, X. Zhu, Z. Wang and B. Xing, *Environ. Sci.: Nano*, 2019, **6**, 1026–1042.
36 S. Du, P. Zhang, R. Zhang, Q. Lu, L. Liu, X. Bao and H. Liu, *Chemosphere*, 2016, **164**, 499–507.
37 B. Lacroix and V. Citovsky, in *Biolistic DNA Delivery in Plants: Methods and Protocols*, eds. S. Rustgi and H. Luo, Springer US, New York, NY, 2020, pp. 125–139.
38 H. Zhang, N. S. Goh, J. W. Wang, R. L. Pinals, E. González-Grandío, G. S. Demirer, S. Butrus, S. C. Fakra, A. Del Rio Flores, R. Zhai, B. Zhao, S.-J. Park and M. P. Landry, *Nat. Nanotechnol.*, 2022, **17**, 197–205.
39 R. Fang, J. Gong, W. Cao, Z. Chen, D. Huang, J. Ye and Z. Cai, *J. Environ. Sci.* , 2022, **112**, 376–387.

View Article Online
DOI: 10.1039/D3EN00268C

40 T. L. Stoiber, M. M. Shafer, D. A. Karner Perkins, J. D. C. Hemming and D. E. Armstrong, *Environ. Toxicol. Chem.*, 2007, **26**, 1563–1571.
41 M. D. Machado and E. V. Soares, *J. Appl. Phycol.*, 2012, **24**, 1509–1516.
42 A. C. Almeida, T. Gomes, K. Langford, K. V. Thomas and K. E. Tollefsen, *Aquat. Toxicol.*, 2017, **189**, 50–59.
43 I. Martín-de-Lucía, M. C. Campos-Mañas, A. Agüera, F. Leganés, F. Fernández-Piñas and R. Rosal, *Environmental Science: Nano*, 2018, **5**, 1729–1744.
44 G. Cheloni and V. I. Slaveykova, *Cytometry A*, 2013, **83**, 952–961.
45 T. C. Haire, C. Bell, K. Cutshaw, B. Swiger, K. Winkelmann and A. G. Palmer, *Front. Plant Sci.*, 2018, **9**, 235.
46 T. Gomes, L. Xie, D. Brede, O.-C. Lind, K. A. Solhaug, B. Salbu and K. E. Tollefsen, *Aquat. Toxicol.*, 2017, **183**, 1–10.
47 M. Terashima, E. S. Freeman, R. E. Jinkerson and M. C. Jonikas, *Plant J.*, 2015, **81**, 147–159.
48 N. H. A. Nguyen, V. V. T. Padil, V. I. Slaveykova, M. Černík and A. Ševců, *Nanoscale Res. Lett.*, 2018, **13**, 159.
49 P. Eullaffroy and G. Vernet, *Water Res.*, 2003, **37**, 1983–1990.
50 P. Mehrshahi, G. T. D. T. Nguyen, A. Gorchs Rovira, A. Sayer, M. Llavero-Pasquina, M. Lim Huei Sin, E. J. Medcalf, G. I. Mendoza-Ochoa, M. A. Scaife and A. G. Smith, *ACS Synth. Biol.*, 2020, **9**, 1406–1417.
51 H. Wu, L. Shabala, S. Shabala and J. P. Giraldo, *Environ. Sci.: Nano*, 2018, **5**, 1567–1583.
52 T. Liu, B. Xiao, F. Xiang, J. Tan, Z. Chen, X. Zhang, C. Wu, Z. Mao, G. Luo, X. Chen and J. Deng, *Nat. Commun.*, 2020, **11**, 2788.
53 J. Kropat, A. Hong-Hermesdorf, D. Casero, P. Ent, M. Castruita, M. Pellegrini, S. S. Merchant and D. Malasarn, *Plant J.*, 2011, **66**, 770–780.
54 G. S. Demirer, H. Zhang, N. S. Goh, E. González-Grandío and M. P. Landry, *Nat. Protoc.*, 2019, **14**, 2954–2971.
55 H. K. Lichtenthaler, in *Methods in Enzymology*, Academic Press, 1987, vol. 148, pp. 350–382.

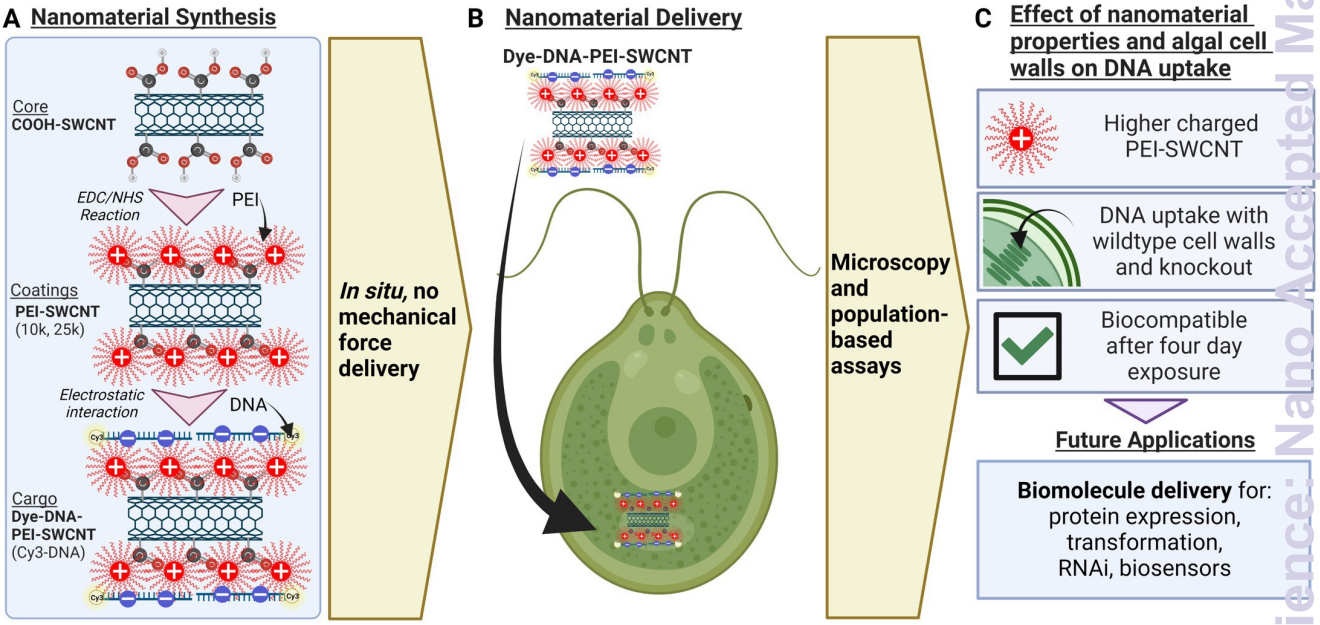

Figure 1. Uptake and impact of single-walled carbon nanotubes (SWCNTs) for DNA delivery in algae. **a)** SWCNTs are functionalized by different molecular weight coatings of polyethylenimine (PEI) and then conjugated with Cy3 dye-labeled single-stranded ssDNA bound for microscopy imaging. **b)** Dye-DNA-PEI-SWCNTs or DNA-PEI-SWCNTs are delivered to *Chlamydomonas reinhardtii* without mechanical aid for colocalization analysis via confocal microscopy or for biocompatibility assays, respectively. **c)** *In situ* uptake of DNA is favored by nanomaterials with higher charge that could be used for multiple synthetic biology and molecular biology research purposes.

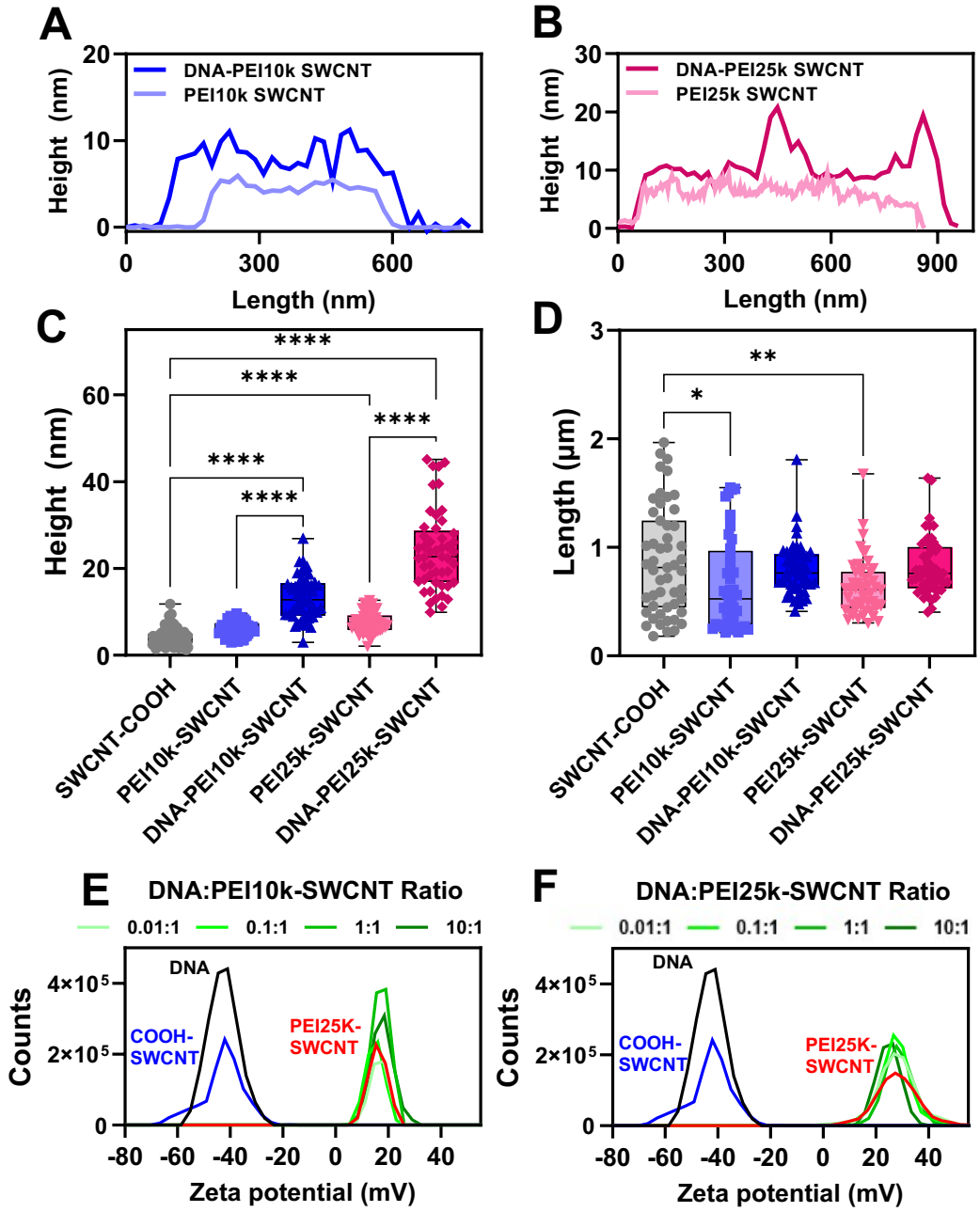

Figure 2. Nanomaterial characterization. a, b) Representative AFM height profiles of PEI10k- and PEI25k-SWCNTs with and without GT15 ssDNA bound at a 1:1 ratio. **c, d)** Average height and length of SWCNT-COOH, PEI10k-/PEI25k- SWCNTs determined from AFM images (*P<0.05, **P<0.01, ****P<0.0001, one way ANOVA, n=50-60). The height of COOH-SWCNT and PEI-SWCNT increased upon coating with PEI and ssDNA, respectively. A slight decrease in length was also observed after coating COOH-SWCNT with PEI by tip sonication. **e, f)** Zeta potential analysis of PEI10k- and PEI25k-SWCNT in the presence of various ssDNA concentrations (10 mM final TE buffer, pH 8.0).

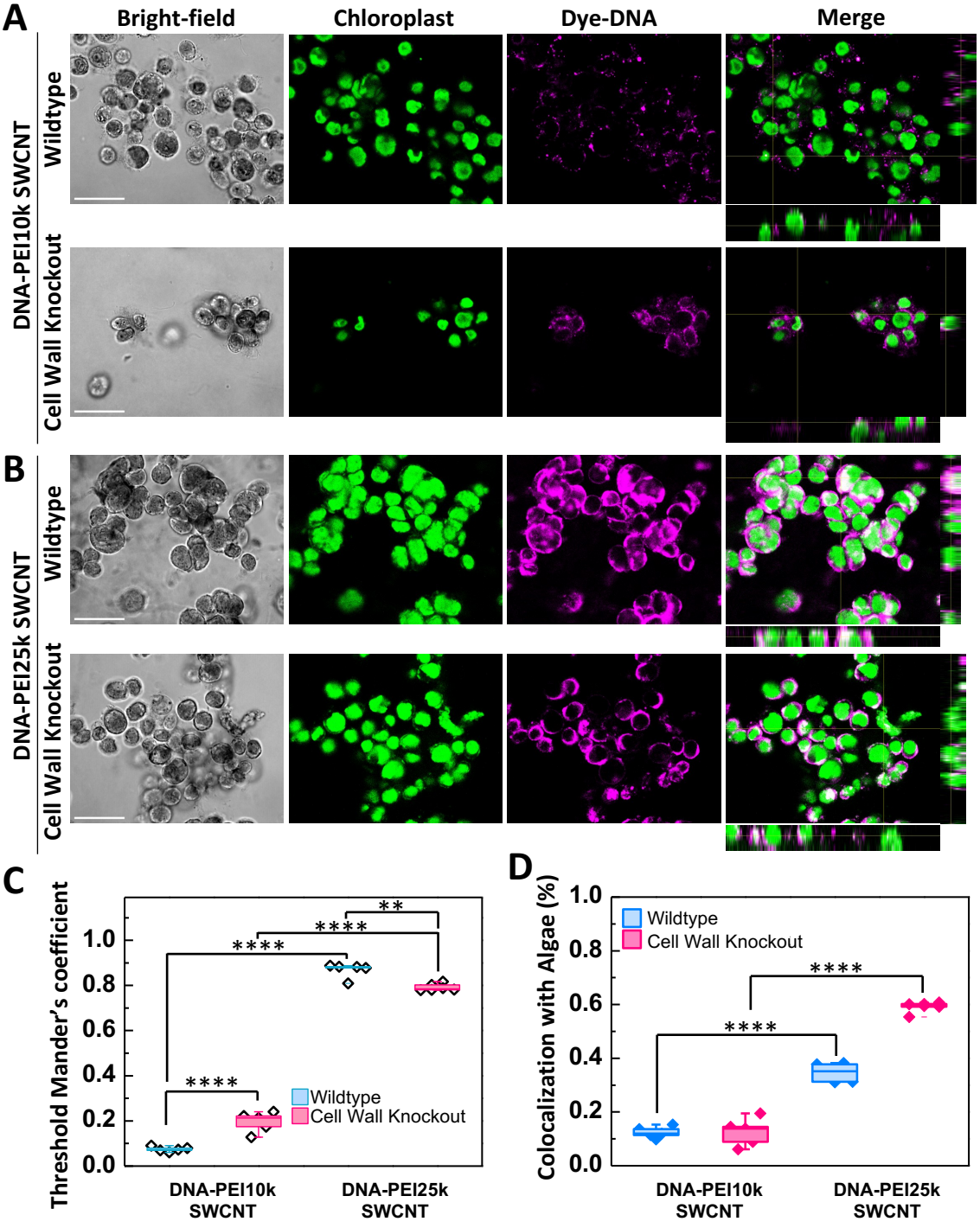

Figure 3. DNA delivery to algal chloroplasts mediated by PEI-SWCNT. Confocal microscopy analysis indicated that **a)** PEI10k-SWCNTs and **b)** PEI25k-SWCNTs have distinct capabilities enhancing the delivery of Cy3 dye-labeled ssGT15 DNA (Dye-DNA) (magenta) into chloroplasts (green) of both wild-type and cell-wall knockout algae strains (1 h incubation, 300 fg/cell PEI-SWCNT, 1:1 Dye-DNA:PEI-SWCNT mass ratio). **c)** Population-based analysis of algae using Mander's colocalization coefficient analysis indicated a statistically significant enhancement in the delivery of Dye-DNA to algae chloroplasts when facilitated by PEI25k-SWCNTs compared to PEI10k-SWCNTs. **d)** Algae cell count analysis demonstrated a higher uptake of Dye-DNA when mediated by PEI25k-SWCNTs compared to PEI10k-SWCNTs in both the wild-type (35.22% ± 3.48 vs. 14.60% ± 2.11) and cell-wall knockout strains (59.20 % ± 2.17 vs. 12.56% ± 5.21). **P<0.01, ****P<0.0001; n=5; 1-way ANOVA analysis; box and whisker plot represents the minimum, 25th percentile, median, 75th percentile, and maximum. The scale bar is 20 μm. Overlaps between Dye-DNA and chloroplasts are highlighted in white in the orthogonal views, which represent projections on the z-axis.

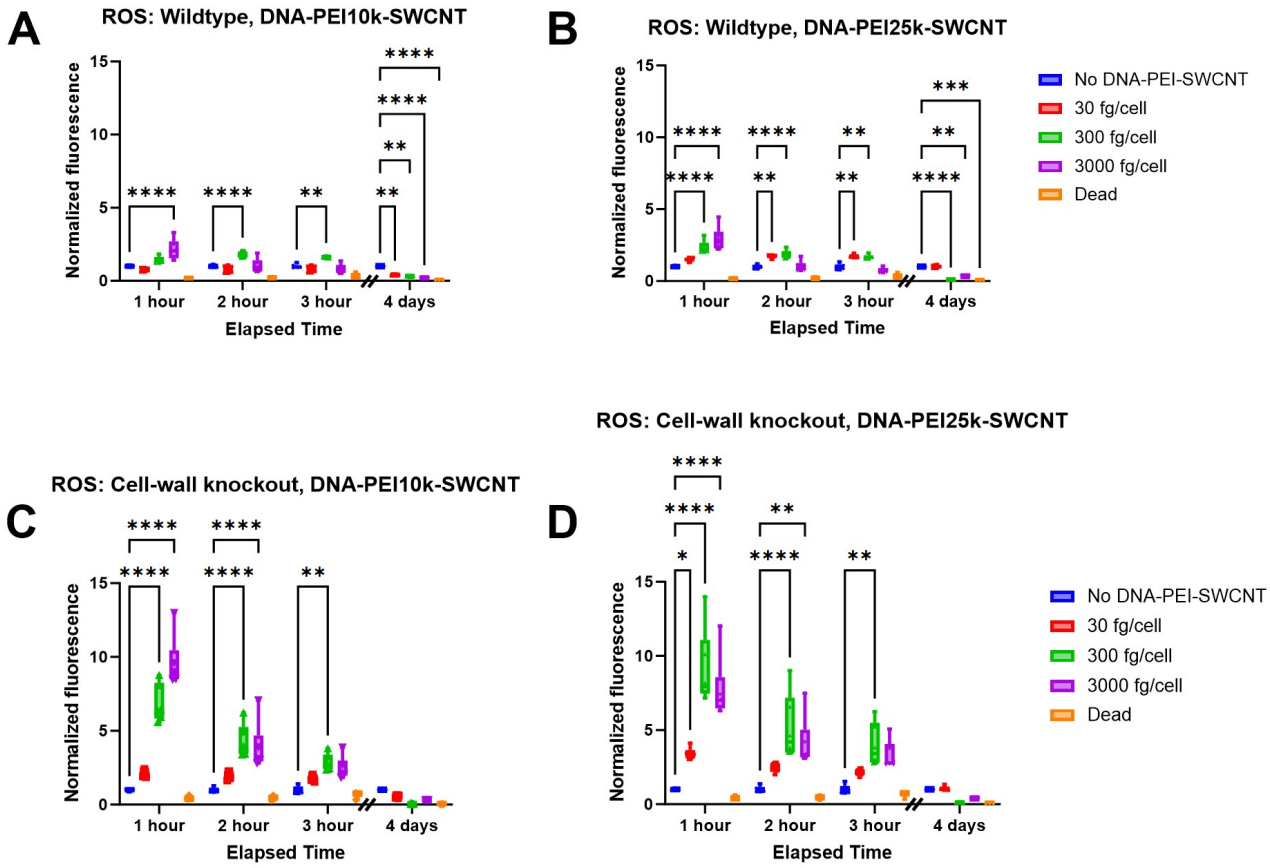

Figure 4. Transient increase in reactive oxygen species (ROS) in *C. reinhardtii* exposed to DNA-PEI-SWCNT. a,b) ROS produced by the wildtype strain peaked with both the DNA-PEI10k-SWCNTs and DNA-PEI25k-SWNTs (3000 fg/cell) at 1 hour and subsequently decreased over time (P****<0.0001, 2-way ANOVA). **c,d)** The cell wall knockout generated higher ROS than the wildtype algae but followed the same trend of peaking at 1 hour, then decreasing for DNA-PEI10k-SWCNTs and DNA-PEI25k-SWCNTs at 30, 300, and 3000 fg/cell (P****<0.0001, P**<0.001, 2-way ANOVA). All samples were normalized to algae-only living cell controls and were done in biological and technical triplicate (N = 3, box and whisker plot represents the minimum, 25th percentile, median, 75th percentile, and maximum).

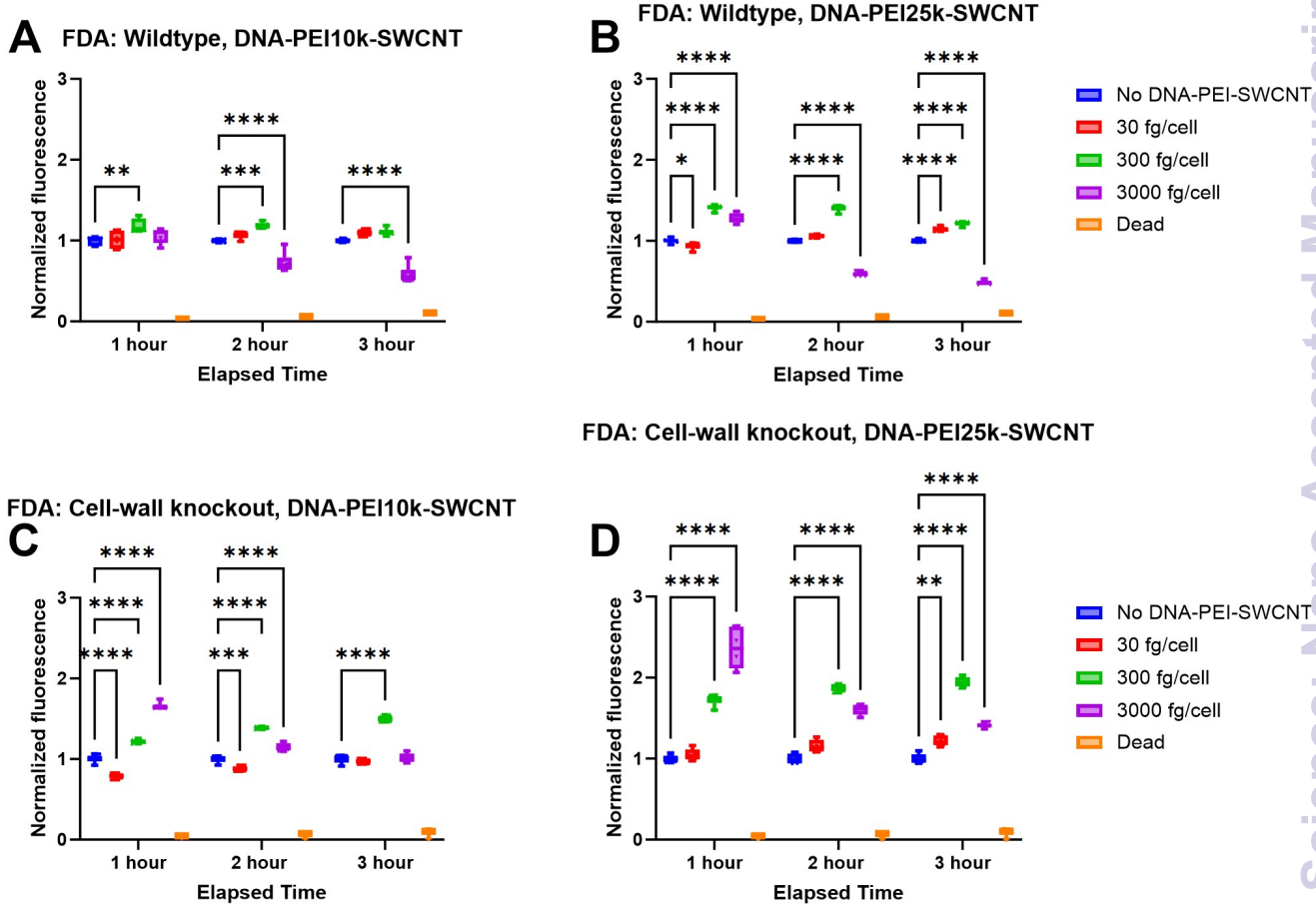

Figure 5. Algae population-based DNA-PEI-SWCNT viability assay for algae with and without a cell wall. a,b) Wildtype algae with cell wall showed decreased viability with DNA-PEI10k-SWCNTs and DNA-PEI25k-SWCNTs at 3000 fg/cell over 2 to 3 hours (P****<0.0001, 2-way ANOVA). **c,d)** The cell wall knockout strain exhibited increases in FDA emission after exposure to DNA-PEI10k-SWCNTs and DNA-PEI25k-SWCNTs at concentrations of 300 and 3000 fg/cell after 1 hour and 2 hours (P****<0.0001, P=0.0998, respectively, 2-way ANOVA). All samples were normalized to algae-only living cell controls and were done in biological and technical triplicate, and no DNA-PEI-SWCNT algae-only wells were used for normalization (N = 3, box and whisker plot represents the minimum, 25th percentile, median, 75th percentile, and maximum).

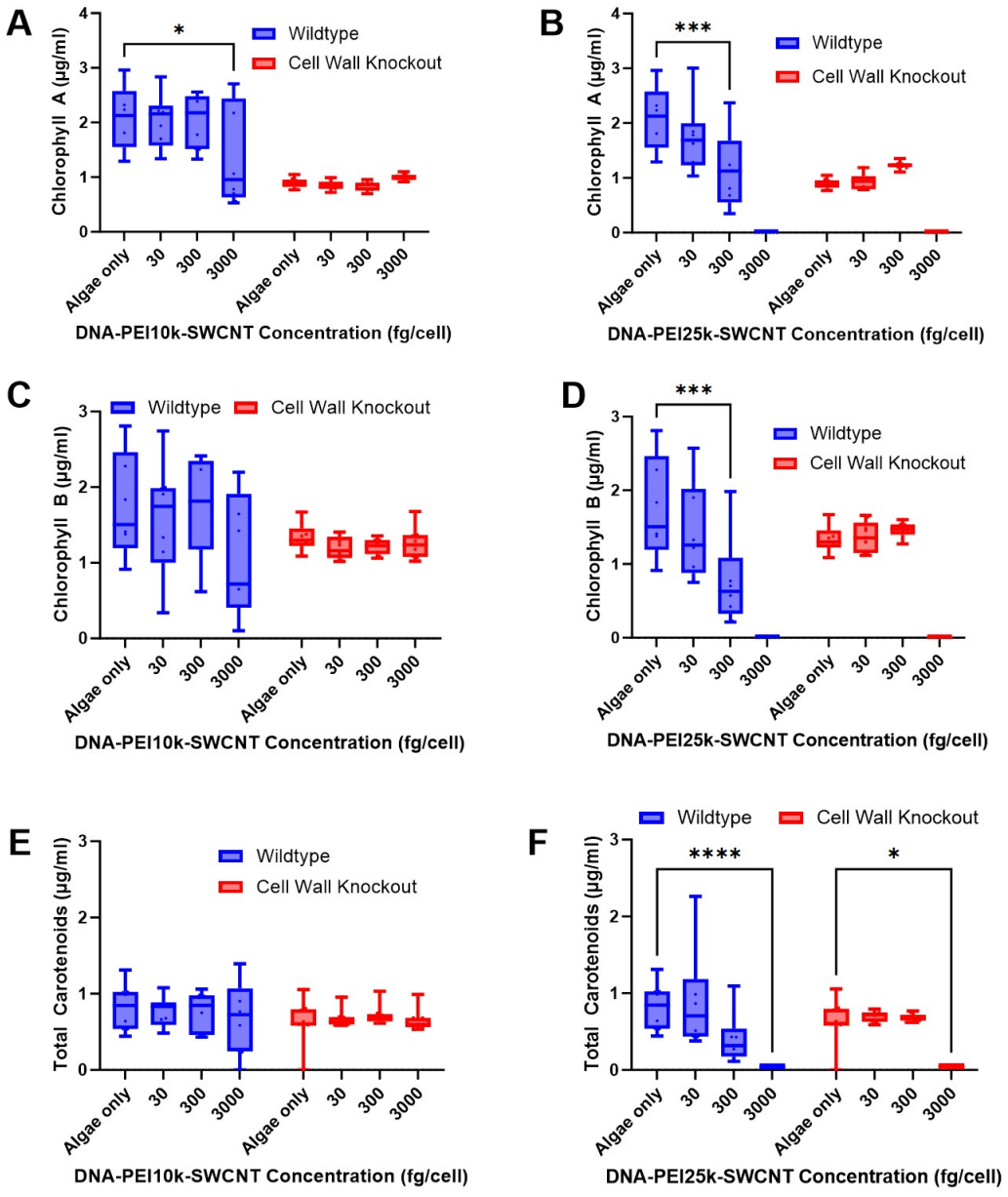

Figure 6. *In vivo* photopigment concentrations for determining biocompatibility of DNA-PEI-SWCNT. Wildtype (CC-124) and the cell-wall knockout strain (CC-4533) were exposed to 1:1 DNA:PEI-SWCNT in microplates under continuous 100 PAR lighting for 4 days. **a)** DNA-PEI10k-SWCNT caused a decrease in chlorophyll *a* in wildtype algae at 3000 fg/cell (*P<0.05) while showing no significant differences in the cell wall knockout. **b**) The wildtype strain showed a reduction in chlorophyll *a* relative to algae-only control at 300 fg/cell DNA-PEI25k-SWCNT (***P<0.005). **c)** No statistically significant difference in chlorophyll *b* was found between the wildtype or cell wall knockout algae when exposed to DNA-PEI10k-SWCNT (P>0.9, 2-way ANOVA). **d**) At 300 fg/cell, DNA-PEI25k-SWCNT showed a statistically significant decrease in chlorophyll *b* (P***=0.0001, 2-way ANOVA) compared to the algae-only control for the wildtype strain, but both strains had no living cells for measurement at 3000 fg/cell, **e)** No differences in total carotenoids were observed after algae exposure to DNA-PEI10k-SWCNTs at different concentrations. **f)** In contrast, wildtype (****P<0.0001) and cell wall knockout (**P<0.003) experienced a decline in total carotenoid content at 3000 fg/cell DNA-PEI25k-SWCNT. Biological triplicates were performed in technical triplicates and assessed with a 2-way ANOVA analysis; box and whisker plot represents the minimum, 25th percentile, median, 75th percentile, and maximum.